Published in final edited form as:
Hypertension. 2009 October ; 54(4): 868–876. doi:10.1161/HYPERTENSIONAHA.109.135152.

Xanthine oxidoreductase depletion induces renal interstitial fibrosis through aberrant lipid and purine accumulation in renal tubules

Toshio Ohtsubo, **Kiyoshi Matsumura**, **Kanae Sakagami**, **Koji Fujii**, **Kazuhiko Tsuruya**, **Hideko Noguchi**, **Ilsa I. Rovira**, **Toren Finkel**, and **Mitsuo Iida**
Department of Medicine and Clinical Science (T.O., K.M., K.S., K.F., K.T., H.N., M.I.), Graduate School of Medical Sciences, Kyushu University, Fukuoka, Japan; and Translational Medicine Branch (I.R., T.F.), National Heart Lung and Blood Institute, National Institutes of Health, Bethesda, MD USA 20892

Abstract

Xanthine oxidoreductase (XOR) is an enzyme responsible for purine degradation, reactive oxygen species (ROS) production and adipogenesis. *XOR* gene disrupted ($XOR^{-/-}$) mice demonstrate renal failure and early death within several months. The aim of this study was to elucidate the mechanism of renal damage in $XOR^{-/-}$ mice and to determine the physiological role of XOR in the kidney. Histological analysis revealed that renal tubular damage in $XOR^{-/-}$ mice was accompanied by deposition of crystals and lipid rich substances. Triglyceride content in renal homogenates was significantly increased in $XOR^{-/-}$ mice. The level of lipogenesis-related gene expression was comparable in $XOR^{+/+}$ and $XOR^{-/-}$ mice, while the expression of adipogenesis-related gene expression was significantly elevated in $XOR^{-/-}$ mice. Urinary excretions of xanthine and hypoxanthine were markedly elevated in $XOR^{-/-}$ mice. Immunohistochemical analysis, Western blotting and real time RT-PCR revealed that various markers of fibrosis, inflammation, ischemia and oxidative stress were increased in $XOR^{-/-}$ mice. Finally, we demonstrate that primary renal epithelial cells from $XOR^{-/-}$ mice are more readily transformed to myofibroblasts, which is a marker of increased epithelial mesenchymal transition. These results suggest that *XOR* gene disruption induced the depletion of uric acid and the accumulation of triglyceride rich substances, xanthine and hypoxanthine in the renal tubules. We believe these changes contribute to a complex cellular milieu characterized by inflammation, tissue hypoxia and ROS production ultimately resulting in renal failure through increased renal interstitial fibrosis.

Keywords

xanthine oxidoreductase; lipid; uric acid; xanthine; renal interstitial fibrosis; epithelial mesenchymal transition; oxidative stress

Introduction

Xanthine oxidoreductase(XOR) was initially identified as the substance in milk which could decolorize methylene blue in 1902[1]. XOR is the enzyme that catalyzes the final two steps in

Correspondence to Toshio Ohtsubo, MD, PhD, Department of Medicine and Clinical Science, Graduate School of Medical Sciences, Kyushu University, Maidashi 3-1-1, Higashi-ku, Fukuoka 812-8582, Japan. Phone: + 81-92-642-5256, Fax: + 81-92-642-5271, tohtsubo@intmed2.med.kyushu-u.ac.jp.

Disclosures
None.

purine catabolism by converting hypoxanthine to xanthine and xanthine to uric acid. Therefore XOR is a key regulator for the production of uric acid.

In addition, XOR has been identified as a critical source of ROS in a variety of pathophysiological conditions such as ischemia/reperfusion injury, hypertension, endothelial dysfunction, atherosclerosis and innate immunity[2–5]. Furthermore, XOR was found to provide pivotal roles in the maturation of antigen-presentingdendritic cells as a source of uric acid[6] and in the biology of the mammary glands, where XOR is a structural component of the membrane-encapsulated milk fat globule[7]. Recently it was shown that XOR is also a novel regulator of adipogenesis and of peroxisome proliferator-activated receptor (PPAR)-γ activity[8]. Thus, XOR has many crucial roles in physiological and pathophysiological functions. However, only about half of all patients with XOR deficiency show xanthine calculi and even less develop an associated arthropathy and myopathy[9].

To elucidate the precise function of *XOR* gene *in vivo*, we developed an *XOR* gene disrupted mice[10]. XOR knockout mice failed to thrive after 10 to 14 days and most die within the first month. Morphological and histological examination in $XOR^{-/-}$mice revealed that obvious changes were detected only in the kidney. Hematoxylin and eosin staining showed that the renal parenchyma was immature with ecstatic to cystic tubules. Similar observations have been made in mice with disruption of the *cyclooxygenase-2 (COX-2)* gene[11,12] and in other mice models of obstructive nephropathy[13]. Serum chemistries revealed that blood urea nitrogen (BUN) in 3-week old $XOR^{-/-}$ mice was elevated at nearly three times compared to those in $XOR^{+/+}$ mice[10]. These and other results suggest that our $XOR^{-/-}$ mice die of renal failure.

In this study we have examined the detailed mechanism of renal injury in $XOR^{-/-}$ mice and discussed the physiological role of the *XOR* gene in the kidney. Disruption of *XOR* gene induced the depletion of uric acid and the accumulation of fat rich deposits and crystals in the renal tubules. Furthermore, fat rich deposits accumulated in the renal tubules with the increased expression of adipogenesis-related genes. These changes might subsequently induce renal tubular dilatation, inflammation, ROS generation and hypoxia of tubular cells. We further demonstrate that these changes ultimately result in renal failure through the expansion of renal interstitial fibrosis.

Methods

Animals

Handling of all animals was done in accordance with prescribed guidelines and ethical approval from the Animal Care and Use Committee of Kyushu University. Experiments were conducted under protocols approved by the Committee of Ethics in Animal Experimentation of the Faculty of Medicine, Kyushu University. Before the animals were euthanized, they were anesthetized with isoflurane (Abbott Japan, Osaka, Japan). Subsequently, blood, urine and tissues were removed and stored at −80°C. Kidney tissues were fixed in alcohol or 4% paraformaldehyde solution.

Blood and urine

Due to their small size, blood samples from 2-week old mice were pooled from 2 to 6 mice and 5 independent samples per group were analyzed. Similary, urine samples from 1-week old mice were pooled from 4 to 6 mice and 4 independent samples were analyzed. Blood and urinary concentrations of xanthine and hypoxanthine were determined using high-performance liquid chromatography[14]. Urinary sediment was prepared from 4-week old $XOR^{+/+}$ and $XOR^{-/-}$ mice (n=3 per group) and analyzed by microscopy.

Preparation of F6 *XOR* gene disrupted mice and genotyping

XOR gene disrupted mice were prepared as described previously[10]. To reduce the renal damage in $XOR^{-/-}$ mice, $XOR^{+/-}$ F1 male mice were mated with C57BL/6J female mice, which is resistant to various renal toxic reagents. Approximately half of $XOR^{-/-}$F6 mice were able to survive until 2 months, but they still remained runted.

Oil Red O staining

Kidney samples were fixed with 4% paraformaldehyde, dehydrated with 10%, 15% and 20% sucrose, subsequently embedded into OCT compound and then stained in Oil Red O solution for 2 min and counterstained with hematoxylin solution.

Lipid contents in kidney

Total lipids from kidney were extracted as described previously[15]. The content was measured using Triglyceride Quantification kit (Wako Chemicals, Osaka, Japan).

Real time reverse transcription-polymerase chain reaction (RT-PCR)

Total RNA was prepared from the cortex of kidney or primary renal epithelial cells using RNeasyProtect Mini kit (Qiagen, Tokyo, Japan). RT-PCR was performed using specific primers (Table S1, please see http://hyper.ahajournals.org), One Step SYBR RT-PCR Kit (Takara-Biomedicals, Otsu, Japan) and LightCycler®2.0 System (Roche Diagnostics KK, Tokyo, Japan).

Immunohistochemistry

Immunohistochemistry was performed as described previously[16,17]. After blocking, kidney sections were subsequently incubated with transforming growth

factor-β (TGF-β) (1:500; Santa Cruz Biotechnology, Santa Cruz, CA, USA), connective tissue growth factor (CTGF) (1:5000; Abcam, Cambridge, UK), α-smooth muscle actin (α-SMA) (1:20; Nichirei, Tokyo, Japan), osteopontin (1:100; Santa Cruz Biotechnology), F4/80 (1:1000; Serotec, Oxford, UK), hypoxia inducible factor-1α (Hif-1α) (1:200; Santa Cruz Biotechnology), 4-hydroxy-2-nonenal (4-HNE) (1:50; NOF Corporation, Tsukuba, Japan) or 8-oxodG (1:100; N45.1; JaICA, Tokyo, Japan) primary antibodies and probed with biotinylated secondary antibody (Nichirei). The sections were incubated with HRP-conjugated streptavidin, visualized by incubating with 3,3′-diaminobenzidine (DAB) and H_2O_2, and counterstained with hematoxylin. At least three different specimens were analyzed. The percentage of positive stained area or cells was analyzed with Image J software. For each kidney, 10 randomly selected fields were analyzed in a blinded manner by a technician without knowledge of the specific background of the study.

Immunohistochemical detection of hypoxic region

Pimonidazole hydrochloride (Hypoxyprobe-1; Chemicon InternationalInc., Temucula, CA, USA) was injected intraperitoneally into XOR mice (60 mg/kg) (n=3 per group)[18]. Thirty minutes after injection, kidneys were quickly removed and fixed in 4% paraformaldehyde solution. Sections were incubated in Hypoxyprobe-1 MAb1 monoclonal antibody (1:50) and treated with biotin-SP-conjugated $F(ab')_2$ fragment of a rabbit anti-mouse IgG (1:500; Accurate Chemical Scientific Corp., Westbury, NY, USA).

Western Blot analysis

Renal cortex was resuspended in RIPA buffer and homogenized using the Mixer Mill MM 300 (Qiagen). Western blotting was performed as described previously[19]. The blocked

nitrocellulose filter was incubated with nitrotyrosine (1:100; Santa Cruz Biotechnology), 4-HNE (1:100) or malondialdehye (MDA) (1:100; NOF Corporation) primary antibodies. The membranes were incubated with the horseradish peroxidase (HRP)-conjugated secondary antibodies and visualized. Blots were stripped in Restore Western Blot Stripping buffer (Pierce Biotechnology Inc., Rockford, IL, USA) and reprobed with GAPDH antibody (1:100; Santa Cruz Biotechnology). The density of signal was analyzed with Image J software. Relative expression of nitrotyrosine and MDA for 1-week old $XOR^{+/+}$ mice was analyzed. Results are presented from 4 mice per group.

Primary culture of renal tubular epithelial cells

Primary renal epithelial cells were prepared by modifying a previously described method[20]. Kidneys from 1-week old XOR mice were dissected to obtain cortical tissue, which was digested with a solutionof 1% type II collagenase (Worthington Biochemical, Lakewood, NJ, USA) and 0.5 mg/ml of soybeantrypsin inhibitor (Invitrogen Japan, Tokyo, Japan) at 37°C for 45 min. The tissue was further dissociated by trituration with a sterile pipette, and then passed through a 100 μm cell strainer (Invitrogen Japan). Cells were grown in a 1:1 serum-free mixture of Dulbecco's Modified Eagle Medium and Ham's F-12 containing15 mM 4-(2-hydroxyethyl)-1-piperazineethanesulfonic acid, 2.5 mM L-glutamine, 50 ng/ml prostaglandin E1, 50 nM hydrocortisone, 40 nM sodium selenite, 10 μg/ml insulin, 5.5 μg/ml transferrin, 50 nM hydrocortisone, 10ng/ml recombinant mouse epidermal growth factor (BioSource, Camarillo, CA, USA), 5 pM 3,3′,5-Triiodo-L-thyronine (reverse T3), 50 U/ml penicillinand 50 μg/ml streptomycin at 37°C. Prostaglandin E1, hydrocortisone and reverse T3 were purchased from Sigma-Aldrich Japan (Tokyo, Japan) and other materials in growing medium were purchased form Invitrogen Japan.

Immunostaining for primary cultured cells

Primary cultures were fixed in 4% paraformaldehyde, treated with 0.5% Triton-X100 and blocked with 3% BSA. The sections were subsequently incubated with TGF-β (1:100), vimentin (1:50; NeoMarkers, Fremont, CA, USA) or E-cadherin (1:1000; BD Transduction Laboratories, San Diego, USA) primary antibodies, probed with secondary antibody and visualized by incubating with DAB and H_2O_2.

Statistical Analysis

Comparisons among age-matched mouse groups were made by Student *t* test and differences between same types of 1-week old and older mouse were analyzed by 1-way ANOVA followed by Bonferroni/Dunn test. Values are expressed as mean ± SEM. Differences were considered statistically significant for $P<0.05$.

Results

Accumulation of triglyceride rich deposits in the renal tubules of $XOR^{-/-}$ mice

The amount of visceral fat appeared to be decreased in $XOR^{-/-}$ mice, while many yellow deposits were found in cross-sectional regions of kidney in 4-week old $XOR^{-/-}$ mice (Figure 1A). To determine whether the yellow deposits contained lipids, Oil Red O staining was performed (Figure 1B). Positive staining was detected in the renal tubules from the cortico-medullary to cortical region of $XOR^{-/-}$ mice, which corresponded with the location of the observed yellow deposits. No staining was detected in $XOR^{+/+}$ mice. The ratio of triglyceride to phospholipid levels in kidney homogenates were significantly elevated in 4-week old $XOR^{-/-}$ mice (Figure 1C).

Expression of lipogenesis and adipogenesis related genes in kidney

To further clarify the mechanism of renal lipid accumulation in $XOR^{-/-}$ mice, the expression of lipogenesis-related genes and adipogenesis-related genes was examined (Table 1). The amount of 3-hydroxy-3-methylglutaryl coenzyme A synthase (HMG-CoA), fatty acid synthase (FAS) and sterol regulatory element-binding protein-1c (SREBP-1c) mRNA was comparable in $XOR^{+/+}$ and $XOR^{-/-}$ mice. On the other hand, the amount of CCAAT/enhancer binding proteins (C/EBP)-α and C/EBP-β mRNA expression was approximately 20- and 50-fold higher in $XOR^{-/-}$ mice, respectively. The relative expression of peroxisome proliferator-activated receptors (PPAR)-α and PPAR-γ in 4-week old $XOR^{-/-}$ mice was also significantly higher than in age-matched $XOR^{+/+}$ mice ($P<0.01$).

Accumulation of crystal deposits in the renal tubules of $XOR^{-/-}$ mice

Blood concentrations of xanthine and hypoxanthine rapidly decreased after birth and reached the lower level of measurement sensitivity (< 0.05 μg/ml) at 4 weeks of age in $XOR^{+/+}$ mice, but were markedly and persistently elevated in $XOR^{-/-}$ mice (Figure 2A). Urinary excretion ratios of xanthine and hypoxanthine to creatinine in 4-week old $XOR^{-/-}$ mice were over 50-fold higher than in age-matched $XOR^{+/+}$ mice (Figure 2B). To verify the deposition of crystals in the renal tubules of $XOR^{-/-}$ mice, we examined the urinary sediment and analyzed the alcohol-fixed renal tissue by polarization. With regards to urinary sediment, 50–100 3m crystals were found in urinary samples from $XOR^{-/-}$ mice (n=3), but no crystals were found in specimens from $XOR^{+/+}$ mice (n=3). Microscopic analysis showed that many brown deposits existed in the dilated renal tubules of $XOR^{-/-}$ mice and polarization verified these deposits were crystals (Figure 2C), but no deposit was detected in the renal tubules of $XOR^{+/+}$ mice (data not shown).

XOR gene disruption induces renal interstitial fibrosis

Masson trichrome staining showed that interstitial fibrosis could be detected around the dilated tubules and aorta of 4-week old $XOR^{-/-}$ mice (Figure 3A). Immunostaining for transforming growth factor-β (TGF-β) and connective tissue growth factor (CTGF), which are key regulators of fibrosis, was performed and positive staining was detected in the cytosol and the nucleus of tubular cells in 4-week old $XOR^{-/-}$ mice, respectively. In addition, immunohistochemical analysis revealed that α-smooth muscle actin (α-SMA), which is a marker of epithelial-mesenchymal transition (EMT), positive staining was detected in both tubuloepithelial and interstitial cells (Figure 3B). These positive stainings in $XOR^{-/-}$ mice were statistically significant compared to those in age-matched $XOR^{+/+}$ mice. The expression levels of TGF-β, α-SMA, vimentin and plasminogen activator inhibitor-1 (PAI-1) mRNA also significantly increased in $XOR^{-/-}$mice when compared to age-matched $XOR^{+/+}$ mice (Table 1).

*XOR*gene deletion induced inflammatory responses, tissue hypoxia and oxidative stress in kidney

Immunoreactivity for osteopontin, an extracellular matrix glycophosphoprotein that induces macrophage infiltration, was detected in the renal epithelial cells of $XOR^{-/-}$ mice at 4 weeks of age (Figure 4A). On the other hand, F4/80 positive cells, which indicate macrophage infiltration, invaded the interstitial spaces between the renal tubules in 4-week old $XOR^{-/-}$ mice. These changes were not observed in 4-week old $XOR^{+/+}$ mice. The amounts of tumor necrosis factor-α (TNF-α), monocyte chemoattractant protein-1 (MCP-1) and gp91phox - one of the NADPH oxidase subunits - mRNA expression were also significantly increased in 4-week old $XOR^{-/-}$ mice when compared to age-matched counterparts ($P<0.01$) (Table 1). To elucidate whether ischemia is involved in renal damage in $XOR^{-/-}$ mice, pimonidazole staining - a marker for tissue hypoxia - was performed in XOR mice. Pimonidazole positive

cells were observed in the segmental region of proximal tubular cells of 4-week old $XOR^{-/-}$ mice. Moreover, hypoxia inducible factor-1α (Hif-1α) positive staining was detected in the nucleus of proximal tubular cells of 4-week old $XOR^{-/-}$ mice. Consistent with an increase in oxidative damage, 4-hydroxy-2-nonenal (4-HNE) positive staining in interstitial cells and 8-oxodG positive staining in the nucleus of interstitial and epithelial cells were detected in 4-week old $XOR^{-/-}$ mice. The amounts of nitrotyrosine, 4-HNE and malondialdehyde (MDA) detected by Western blot analysis were decreased after birth until 2-week old $XOR^{+/+}$ and $XOR^{-/-}$ mice. However, accumulation of nitrotyrosine and MDA in 4- and 8-week old $XOR^{-/-}$ mice was significantly increased compared to age-matched $XOR^{+/+}$ mice (Figure 4B).

XOR gene deletion facilitates renal epithelial-mesenchymal transition

Our results suggest that *XOR* gene deletion might potentiate epithelial-mesenchymal transition (see Figure 3B). To assess whether this is a cell-autonomous effect, primary renal epithelial cells were prepared. Histological examination revealed that primary renal epithelial cells from $XOR^{-/-}$ mice changed morphology from a cuboidal to a fibroblastic shape. Immunohistochemical analysis also showed that positive staining for TGF-β and vimentin was only detected in primary cells isolated from $XOR^{-/-}$ mice, while the regions of fibroblastic shaped cells in $XOR^{-/-}$ mice were not stained with anti-E-cadherin antibody (Figure 5A). Furthermore, the amount of TGF-β, vimentin and α-SMA mRNA expression were also significantly increased in $XOR^{-/-}$ mice ($P<0.01$) (Figure 5B).

Discussion

In the present study we describe the possible pathways involved in renal injury in $XOR^{-/-}$ mice. Disruption of the *XOR* gene induced the accumulation of triglyceride rich lipids in the renal tubules with the increased expression of adipogenesis-related genes. Moreover, *XOR* gene deletion inhibits the conversion from hypoxanthine to xanthine and xanthine to uric acid, resulting in increases in hypoxanthine and xanthine concentrations in blood and urine and subsequent deposition of insoluble crystals in the renal tubules. These deposits in the renal tubule we believe can trigger inflammation, decreased renal blood flow and increased ROS production in spite of *XOR* gene disruption. In fact, the amounts of oxidative products were similar in both $XOR^{+/+}$ and $XOR^{-/-}$ mice until 2-week old. However, accumulation of oxidative products were significantly increased in 4-week old $XOR^{-/-}$ mice (Figure 4B) accompanying with the increase in xanthine and hypoxanthine concentrations in blood (Figure 2A) and the augmented excretion of xanthine in urine (Figure 2B). Furthermore, since uric acid is known to possess strong antioxidant properties[21,22], the absence of uric acid might also accelerate the accumulation of ROS and aggravated renal injury. As such, it would seem that these observed alterations in $XOR^{-/-}$ mice might combine to induce interstitial fibrosis following EMT and ultimately lead to renal failure.

Xanthinuria is a rare hereditary disorder of purine metabolism resulting from a deficiency of the XOR enzyme in humans[9]. Patients with *XOR* gene deficiency rarely suffer from renal failure. In contrast, $XOR^{-/-}$ mice die of renal failure several weeks after birth, indicating that XOR plays a pivotal role during postnatal renal maturation in mice. Three reasons may explain the different progression of renal damage observed in humans and mice with *XOR* gene deficiencies. First, the role of XOR protein in mice might be more important than in humans because XOR enzyme activity in mice is 100 times higher than that in human[23]. Second, urinary concentration of xanthine, which is less soluble than uric acid, is approximately one hundred-fold higher in $XOR^{-/-}$mice than in xanthinuria patients[9], suggesting that high levels of xanthine might contribute to renal damage in mice. There might also be differences in purine catabolism between mice and human with *XOR* gene deletion. For example, mice express the uricase enzyme to catalyze the metabolism of uric

acid to allantoin, which is more soluble in water, but humans have lost this enzyme's activity during evolution[24]. On the other hand, the hypoxanthine salvage pathway in hereditary xanthinuria is enhanced to reduce the amount of hypoxanthine[25], suggesting that the hypoxanthine salvage pathway in humans may have developed to compensate for the loss of uricase activity. Third, humans with *XOR* gene deletions can use the XOR protein derived from their mother during pregnancy, and their kidneys are fully matured at birth. Meanwhile, mouse fetuses with *XOR* gene deletions are also capable of using XOR derived from their mother during pregnancy, but cannot use the XOR protein to mature kidney, because mice need 16 days after birth for kidney maturation[26]. Despite these important differences, we believe our model provides a useful genetic system to explore the physiological role of xanthine oxidase.

It has been reported that renal triglyceride contents increase and deposit in the renal tubular and glomerular cells to protect the renal tissue against various types of renal damage[27]. High fat diet also increases plasma triglycerides and cholesterol, and induces marked neutral lipids accumulation in both the glomerular and tubulointerstitial lesions[28,29]. In this study, the kidney homogenates of $XOR^{-/-}$ mice contained significantly higher triglyceride levels when compared to their counterparts (Figure 1C). On the other hand, lipid deposition was not found in the renal epithelial cells, glomerular cells or tubulointerstitial cells but was detected within the renal tubule. It has been reported that XOR protein is usually present in the peritubular region, but in case of hyperlipidemia, XOR is detected in the tubular epithelium[30]. There is evidence that XOR is one of the regulators of adipogenesis and PPAR-γ activity in preadipocytes, and inhibition of XOR expression and/or enzymatic activity blocks both PPARγ activation and adipocyte differentiation[8]. These results suggest that XOR or its products in renal epithelial cells may play a role in protecting them from damage by regulating adipogenesis and redox state. Further experiments will be required to clarify the detailed mechanism by which XOR regulates adipogenesis in kidney.

EMT plays an important role in the progression of interstitial fibrosis in the kidney[31]. Immunostaining for α-SMA antibody demonstrated positive staining consistent with the accumulation of myofibroblasts (Figure 3). Increased expression of both TGF-β and CTGF protein, which are the main inducers of EMT, was also detected in $XOR^{-/-}$ mice. These results suggest that EMT participates in the progression of renal damage in $XOR^{-/-}$ mice. Furthermore, primary renal epithelial cells prepared from $XOR^{-/-}$ mice transformed to myofibroblasts and demonstrate increased expression of TGF-β, vimentin and α-SMA (Figure 5). Together these observations suggest that *XOR* gene disruption in renal epithelial cells facilitates the EMT. The reason for this phenomenon remains unclear, but a decrease in antioxidant capacity with loss of uric acid, or alteration of renal lipid homeostasis in $XOR^{-/-}$ mice might be involved in this alteration in the EMT.

In the past several years, evidence has been accumulated that hyperuricemia is associated with metabolic syndrome, cardiovascular events, hypertension, stroke, diabetes mellitus and chronic kidney disease[32,33]. Furthermore, lowering uric acid with the use of XOR inhibitor can improve the progression of renal disease, ischemic injuries, inflammatory diseases, and chronic heart failure[34–36]. On the other hand, several large cohort studies showed that hypouricemia as well as hyperuricemia were also associated with cardiovascular disease, stroke and chronic kidney disease in subjects with hypertension or diabetes, in addition to the general population[37–39]. It has been reported that uric acid has antioxidant activity against a variety of oxidants[21,22]. These results suggest that hyperuricemia may be in part a compensatory mechanism to counteract oxidative damage. There must be an optimal concentration of uric acid in blood and the role of uric acid may be different in various physiological and pathophysiological conditions. In addition, it has been assumed that XOR protein is one of the major sources of ROS and worsens the oxidative injury, but complete

deletion of XOR protein induced accumulation of oxidative products and renal injury. In some tissues under pathophysiological conditions, increased XOR activity may therefore be an adaptive response to produce uric acid and reduce oxidative stress.

Supplementary Material

Refer to Web version on PubMed Central for supplementary material.

Acknowledgments

Sources of Funding

This work was supported in part by Grants-in-Aid for Scientific Research from the Ministry of Education, Science, Sports and Culture of Japan, 19590954.

References

1. Schardinger F. Ueber das Verhalten der Kuhmilch gegen Methylblau und seine Verwendung zur Unterscheidung von ungekochter und gekochter Milch. Z Untersuch Nahrungs Genussmittel. 1902; 5:1113–1121.
2. Harrison R. Structure and function of xanthine oxidoreductase: where are we now. Free Radic Biol Med. 2002; 33:774–797. [PubMed: 12208366]
3. Meneshian A, Bulkley GB. The physiology of endothelial xanthine oxidase: from urate catabolism to reperfusion injury to inflammatory signal transduction. Microcirculation. 2002; 9:161–175. [PubMed: 12080414]
4. Granger DN, Rutili G, McCord JM. Superoxide radicals in feline intestinal ischemia. Gastroenterology. 1981; 81:22–29. [PubMed: 6263743]
5. Vorbach C, Harrison R, Capecchi MR. Xanthine oxidoreductase is central to the evolution and function of the innate immune system. Trends Immunol. 2003; 24:512–517. [PubMed: 12967676]
6. Shi Y, Evans JE, Rock KL. Molecular identification of a danger signal that alerts the immune system to dying cells. Nature. 2003; 425:516–521. [PubMed: 14520412]
7. McManaman JL, Palmer CA, Wright RM, Neville MC. Functional regulation of xanthine oxidoreductase expression and localization in the mouse mammary gland: evidence of a role in lipid secretion. J Physiol. 2002; 545:567–579. [PubMed: 12456835]
8. Cheung KJ, Tzameli I, Pissios P, Rovira I, Gavrilova O, Ohtsubo T, Chen Z, Finkel T, Flier JS, Friedman JM. Xanthine oxidoreductase is a regulator of adipogenesis and PPARgamma activity. Cell Metab. 2007; 5:115–128. [PubMed: 17276354]
9. Ichida K, Amaya Y, Kamatani N, Nishino T, Hosoya T, Sakai O. Identification of two mutations in human xanthine dehydrogenase gene responsible for classical type I xanthinuria. J Clin Invest. 1997; 99:2391–2397. [PubMed: 9153281]
10. Ohtsubo Y, Rovira II, Starost MF, Liu C, Finkel T. Xanthine oxidoreductase is an endogeneous regulator of cyclooxygenase-2. Circ Res. 2004; 95:1118–1124. [PubMed: 15528468]
11. Dinchuk JE, Car BD, Focht RJ, Johnston JJ, Jaffee BD, Covington MB, Contel NR, Eng VM, Collins RJ, Czerniak PM, Gorry SA, Trzaskos JM. Renal abnormalities and an altered inflammatory response in mice lacking cyclooxygenase II. Nature. 1995; 378:406–409. [PubMed: 7477380]
12. Morham SG, Langenbach R, Loftin CD, Tiano HF, Vouloumanos N, Jennette JC, Mahler JF, Kluckman KD, Ledford A, Lee CA, Smithies O. Prostaglandin synthase 2 gene disruption causes severe renal pathology in the mouse. Cell. 1995; 83:473–482. [PubMed: 8521477]
13. Klahr S, Morrissey J. Obstructive nephropathy and renal fibrosis. Am J Physiol Renal Physiol. 2002; 283:F861–F875. [PubMed: 12372761]
14. Anderson FS, Murphy RC. Isocratic separation of some purine nucleotide, nucleoside, and base metabolites from biological extracts by high-performance liquid chromatography. J Chromatogr. 1976; 121:251–262. [PubMed: 6484]

15. Bligh E, Dyer W. A rapid method of total lipid extraction and purification. Can J Biochem Physiol. 1959; 37:911–917. [PubMed: 13671378]
16. Tsuruya K, Furuichi M, Tominaga Y, Shinozaki M, Tokumoto M, Yoshimitsu T, Fukuda K, Kanai H, Hirakata H, Iida M, Nakabeppu Y. Accumulation of 8-oxoguanine in the cellular DNA and the alteration of the OGG1 expression during ischemia-reperfusion injury in the rat kidney. DNA Repair. 2003; 2:211–229. [PubMed: 12531391]
17. Ohtsubo T, Ohya Y, Nakamura Y, Kansui Y, Furuichi M, Matsumura K, Fujii K, Iida M, Nakabeppu Y. Accumulation of 8-oxo-deoxyguanosine in cardiovascular tissues with the development of hypertension. DNA Repair. 2007; 6:760–769. [PubMed: 17280880]
18. Morani A, Arros BRP, Imamov O, Hultenby K, Arner A, Warner M, Gustafsson JA. Lung dysfunction causes systemic hypoxia in estrogen receptor β knockout (ERβ$^{-/-}$) mice. Proc Natl Acad Sci USA. 2006; 103:7165–7169. [PubMed: 16636272]
19. Ohtsubo T, Nishioka K, Imaiso Y, Iwai S, Shimokawa H, Oda H, Fujiwara T, Nakabeppu Y. Identification of human MutY homolog (hMYH) as a repair enzyme for 2-hydroxyadenine in DNA and detection of multiple forms of hMYH located in nuclei and mitochondria. Nucleic Acids Res. 2000; 28:1355–1364. [PubMed: 10684930]
20. Terryn S, Jouret F, Vandenabeele F, Smolders I, Moreels M, Devuyst O, Steels P, Van Kerkhove E. A primary culture of mouse proximal tubular cells, established on collagen-coated membranes. Am J Physiol Renal Physiol. 2007; 293:F476–F485. [PubMed: 17475898]
21. Kean RB, Spitsin SV, Mikheeva T, Scott GS, Hooper DC. The peroxynitrite scavenger uric acid prevents inflammatory cell invasion into the central nervous system in experimental allergic encephalomyelitis through maintenance of blood-central nervous system barrier integrity. J Immunol. 2000; 165:6511–6518. [PubMed: 11086092]
22. Ames BN, Cathcart R, Schwiers E, Hochstein P. Uric acid provides an antioxidant defense in humans against oxidant- and radical-caused aging and cancer: a hypothesis. Proc Natl Acad Sci USA. 1981; 78:6858–6862. [PubMed: 6947260]
23. Xu P, Vallee PL, Hoidal JR. Repressed expression of the human xanthine oxidoreductase gene. J Biol Chem. 2000; 275:5918–5926. [PubMed: 10681584]
24. Yelandi AV, Chu R, Pan J, Zhu Y, Usuda N. Peroxisomal Purine Metabolism. Ann N Y Acad Sci. 1996; 804:165–175. [PubMed: 8993543]
25. Mateos FA, Puig JG, Jimenez ML, Fox IH. Hereditary xanthinuria. Evidence for enhanced hypoxanthine salvage. J Clin Invest. 1987; 79:847–852. [PubMed: 3818951]
26. Koseki C, Herzlinger D, Al-Awqati Q. Apoptosis in metanephric development. J Cell Biol. 1992; 119:1327–1333. [PubMed: 1447305]
27. Zager RA, Johnson AC, Hanson SY. Renal tubular triglyercide accumulation following endotoxic, toxic, and ischemic injury. Kidney Int. 2005; 67:111–121. [PubMed: 15610234]
28. Kume S, Uzu T, Araki S, Sugimoto T, Isshiki K, Chin-Kanasaki M, Sakaguchi M, Kubota N, Terauchi Y, Kadowaki T, Haneda M, Kashiwagi A, Koya D. Role of altered renal lipid metabolism in the development of renal injury induced by a high-fat diet. J Am Soc Nephrol. 2007; 18:2715–2723. [PubMed: 17855643]
29. Gwinner W, Scheuer H, Haller H, Brandes RP, Groene HJ. Pivotal role of xanthine oxidase in the initiation of tubulointerstitial renal injury in rats with hyperlipidemia. Kidney Int. 2006; 69:481–487. [PubMed: 16407880]
30. Pfeffer KD, Hueckstead TP, Hoidal JR. Xanthine dehydrogenase and xanthine oxidase activity and gene expression in renal epithelial cells. Cytokine and steroid regulation. J Immunol. 1994; 153:1789–1797. [PubMed: 8046245]
31. Liu Y. Epithelial to mesenchymal transition in renal fibrogenesis: pathologic significance, molecular mechanism, and therapeutic intervention. J Am Soc Nephrol. 2004; 15:1–12. [PubMed: 14694152]
32. Johnson RJ, Kang DH, Feig D, Kivlighn S, Kanellis J, Watanabe S, Tuttle KR, Rodriguez-Iturbe B, Herrera-Acosta J, Mazzali M. Is there a pathogenetic role for uric acid in hypertension and cardiovascular and renal disease? Hypertension. 2003; 41:1183–1190. [PubMed: 12707287]

33. Nakagawa T, Kang DH, Feig D, Sanchez-Lozada LG, Srinivas TR, Sautin Y, Ejaz AA, Segal M, Johnson RJ. Unearthing uric acid: an ancient factor with recently found significance in renal and cardiovascular disease. Kidney Int. 2006; 69:1722–1725. [PubMed: 16598194]

34. Siu YP, Leung KT, Tong MK, Kwan TH. Use of allopurinol in slowing the progression of renal disease through its ability to lower serum uric acid level. Am J Kidney Dis. 2006; 47:51–59. [PubMed: 16377385]

35. Pacher P, Nivorozhkin A, Szabo C. Therapeutic effects of xanthine oxidase inhibitors: renaissance half a century after the discovery of allopurinol. Pharmacol Rev. 2006; 58:87–114. [PubMed: 16507884]

36. Hajjar RJ, Leopold JA. Xanthine oxidase inhibition and heart failure: novel therapeutic strategy for ventricular dysfunction? Circ Res. 2006; 98:169–171. [PubMed: 16456108]

37. Verdecchia P, Schillaci G, Reboldi G, Santeusanio F, Porcellati C, Brunetti P. Relation between serum uric acid and risk of cardiovascular disease in essential hypertension. The PIUMA study. Hypertension. 2000; 36:1072–1078. [PubMed: 11116127]

38. Lehto S, Niskanen L, Ronnemaa T, Laakso M. Serum uric acid is a strong predictor of stroke in patients with non-insulin-dependent diabetes mellitus. Stroke. 1998; 29:635–639. [PubMed: 9506605]

39. Suliman ME, Johnson RJ, García-López E, Qureshi AR, Molinaei H, Carrero JJ, Heimbürger O, Bárány P, Axelsson J, Lindholm B, Stenvinkel P. J-shaped mortality relationship for uric acid in CKD. Am J Kidney Dis. 2006; 48:761–771. [PubMed: 17059995]

Perspectives

We examined the physiological role of XOR in the kidney using an *XOR* knockout mouse model and showed possible roles for this protein. The *XOR* gene might be essential for kidney maturation and survival of mice during the postnatal period via the regulation of fat and purine metabolism. The *XOR* gene may regulate adipogenesis in the kidney and have a pivotal role in preventing the epithelial cells from transforming to mesenchymal cells.

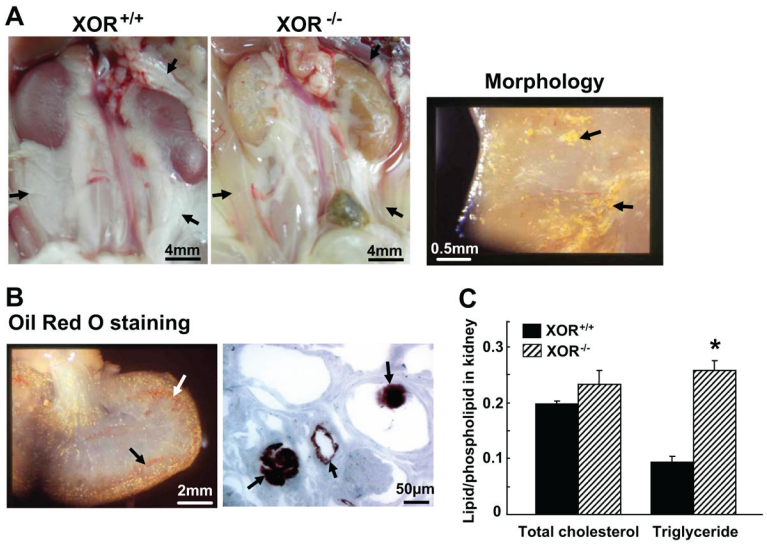

Figure 1.

XOR gene disruption altered lipid homeostasis and accumulation of triglyceride rich deposits in kidney. A, Reduced visceral fat content (arrows) and pale yellow color of kidney in 4-week old $XOR^{-/-}$ mice (left) (n=16). Morphology of kidney in 4-week old $XOR^{-/-}$ mice (right) (n=4). Arrows show yellow deposits. B, Oil Red O staining of kidney in 4-week old $XOR^{-/-}$ mice (n=4). Arrows show Oil Red O positive staining. C, Ratio of total cholesterol and triglyceride to phospholipid in kidney at 4-week old XOR mice. Each bar represents the mean ± SEM from 6 mice per group. *P<0.001 compared with $XOR^{+/+}$ mice.

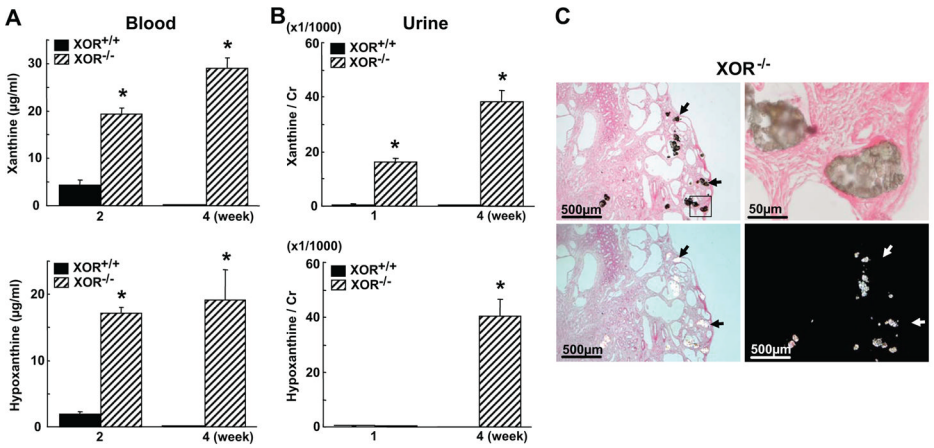

Figure 2.

Disruption of *XOR* gene induces the accumulation of crystals in the renal tubules. A, Blood concentration of xanthine and hypoxanthine. *P<0.001 compared with age-matched $XOR^{+/+}$ mice. Blood samples from 2-week old mice were pooled from 2 to 6 mice and 5 independent samples per group were analyzed. Eight samples of 4-week old mice were used. Values are means ± SEM. B, Ratio of urinary xanthine and hypoxanthine to creatinine. *P<0.001 compared with age-matched $XOR^{+/+}$ mice. Urine samples from 1-week old mice were pooled from 4 to 6 mice and 4 independent samples were analyzed. Seven samples at 4-week old mice were used. Values are means ± SEM. C, Microscopic view of dilated renal tubules containing brown material (upper) and white deposit (lower) by polarization in the cortex (n=3 mice per group). Arrows show deposits.

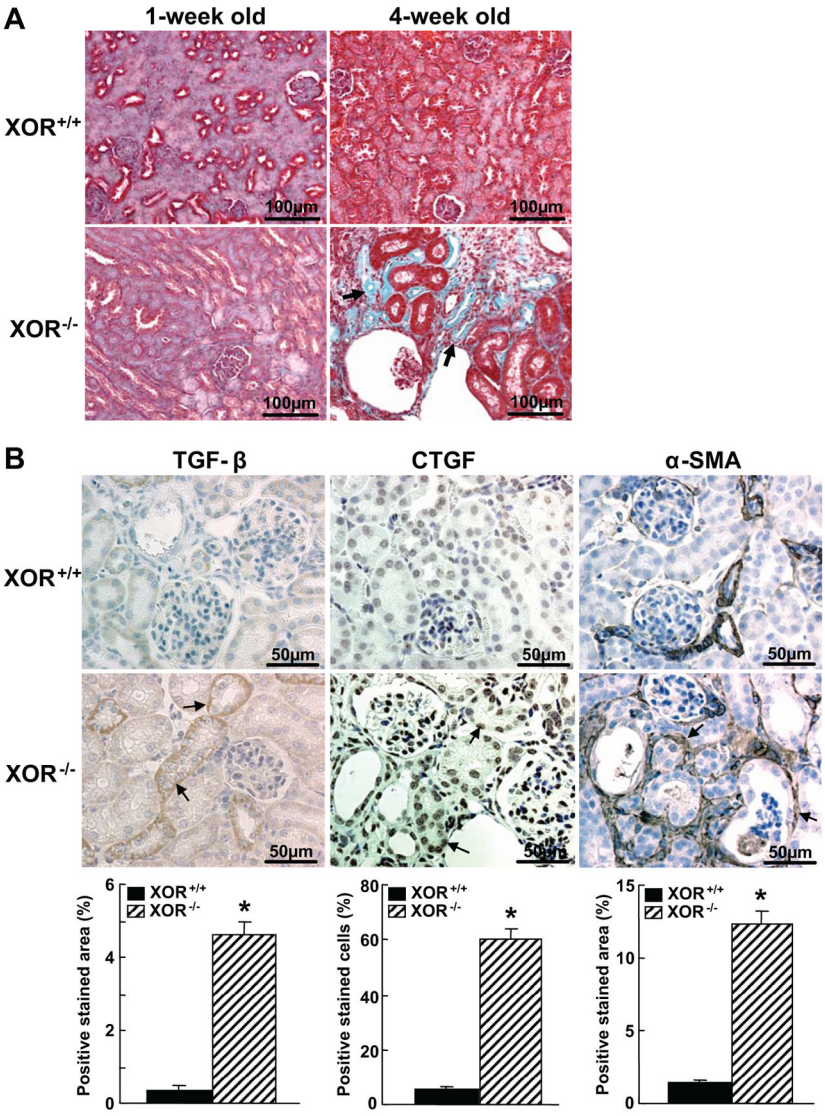

Figure 3.

Disruption of *XOR* gene induces renal interstitial fibrosis. A, Masson trichrome staining in the kidney of 1- and 4-week old $XOR^{+/+}$ and $XOR^{-/-}$ mice (n=3 per each group). Arrows show positive regions. B, Immunohistochemical analysis of TGF-β, CTGF and α-SMA expression in 4-week old $XOR^{+/+}$ and $XOR^{-/-}$ mouse kidneys (n=3 per group) (upper panel). Arrows show positive regions. Percentage of positive stained area for TGF-β and α-SMA, and positive stained cells for CTGF (lower panel). Each bar represents the mean ± SEM from 3 mice per group. For each mouse, 10 randomly selected fields were analyzed. *P<0.01 compared with $XOR^{+/+}$ mice.

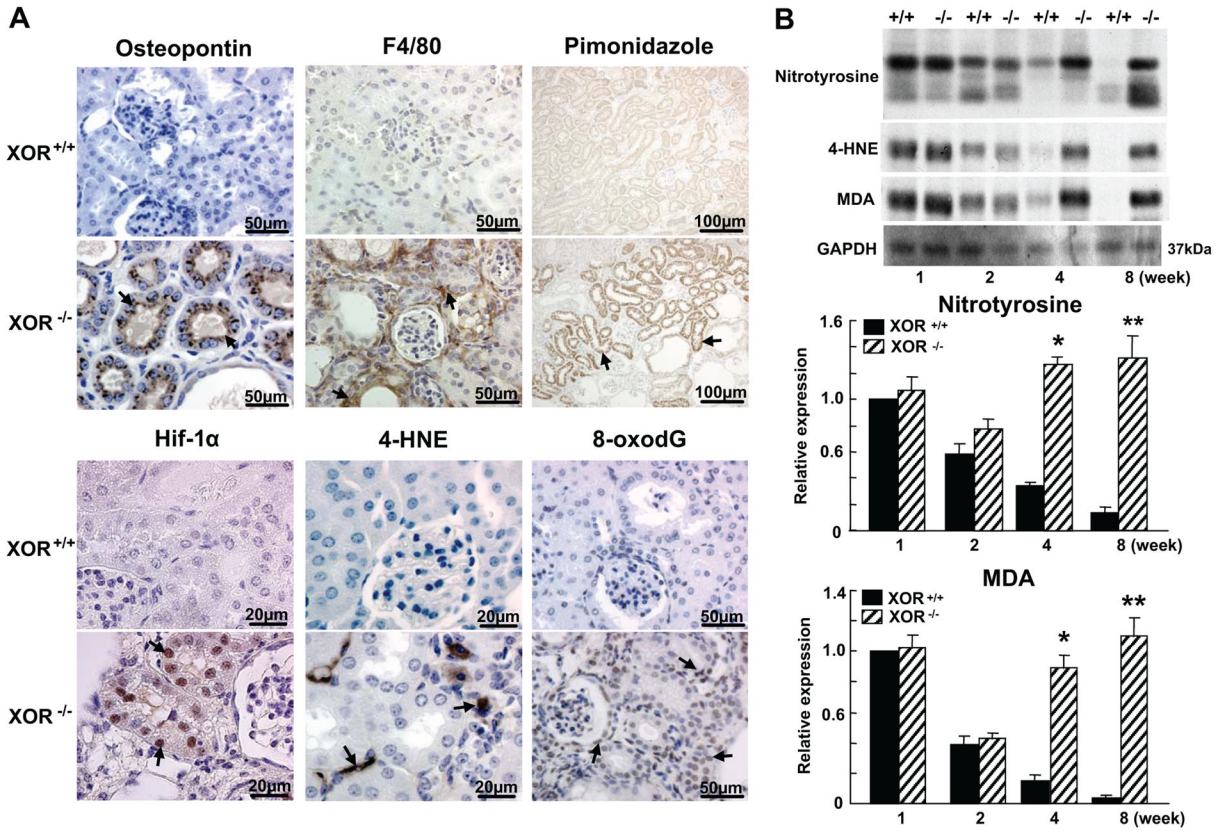

Figure 4.

XOR gene depletion induced inflammation, hypoxia and oxidative stress in kidney. A, Immunostaining for osteopontin, F4/80, pimonidazole, Hif-1α, 4-HNE and 8-oxodG positive cells in 4-week old $XOR^{+/+}$ and $XOR^{-/-}$ mice (n=3 per group). Arrows show positive regions. B, Representative Western blot shows the time course of nitrotyrosine, 4-HNE, MDA and GAPDH expression in the cortex of kidney in $XOR^{+/+}$ and $XOR^{-/-}$ mice (left). +/+: $XOR^{+/+}$ mice, −/−: $XOR^{-/-}$ mice. Relative expression of nitrotyrosine and MDA for 1 week-old $XOR^{+/+}$ mice is shown (right). Results are presented as the mean ± SEM from 4 mice per group. *P<0.01 and **P<0.001 compared with age-matched $XOR^{+/+}$ mice.

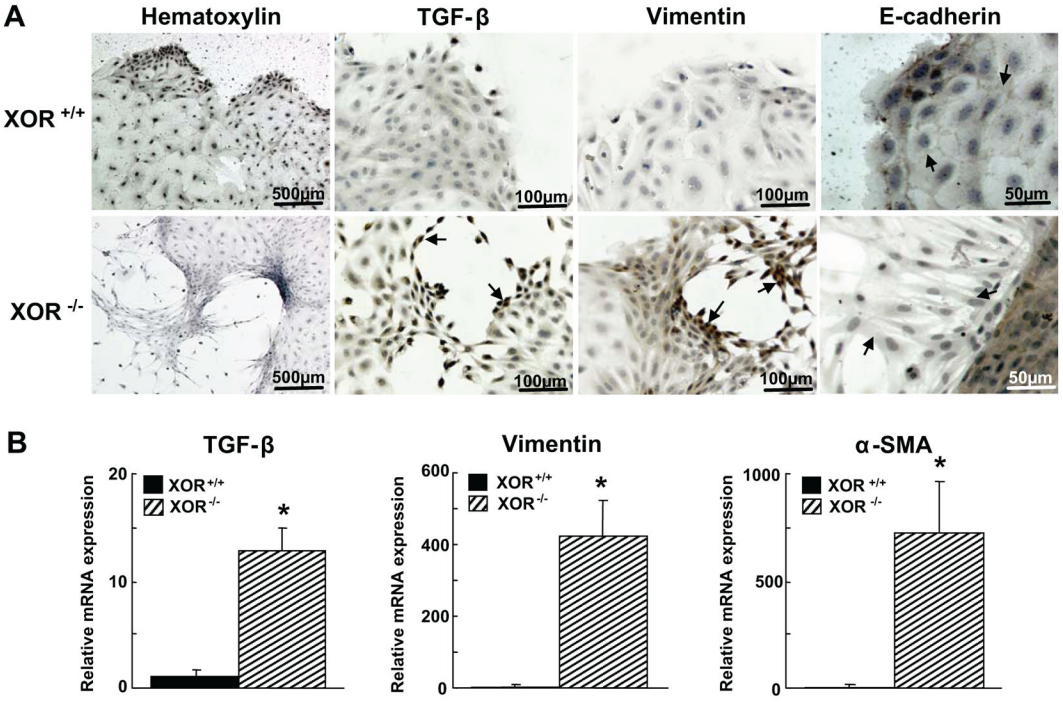

Figure 5.

XOR gene disruption facilitates renal epithelial-mesenchymal transition. A, Hematoxylin staining of primary renal epithelial cells from $XOR^{+/+}$ and $XOR^{-/-}$ mice(n=3). Immunostaining for TGF-β, vimentin and E-cadherin in primary renal epithelial cells from $XOR^{+/+}$ and $XOR^{-/-}$ mice (n=3). Arrows show positive region. B, Amounts of TGF-β, vimentin and α-SMA mRNA expression in primary renal epithelial cells from $XOR^{+/+}$ and $XOR^{-/-}$ mice. Each bar represents the mean ± SEM from 6 mice per group. *P<0.01 compared with $XOR^{+/+}$ mice.

Table 1

Relative mRNA expression to GAPDH in kidney of 4-week old XOR mice

Gene	$XOR^{+/+}$	$XOR^{-/-}$
Lipogenesis		
HMG-CoA	1 ± 0.54	2.58 ± 1.01
FAS	1 ± 0.21	1.51 ± 0.3
SEBP-1c	1 ± 0.39	2.42 ± 0.99
Adipogenesis		
C/EBP-α	1 ± 0.12	21.0 ± 8.45 *
C/EBP-β	1 ± 0.45	49.8 ± 16.4 *
PPAR-α	1 ± 0.29	7.49 ± 1.49 *
PPAR-γ	1 ± 0.16	5.73 ± 1.23 *
Fibrosis		
TGF-β	1 ± 0.08	25.2 ± 2.12 *
α-SMA	1 ± 0.27	123 ± 29.9 *
Vimentin	1 ± 0.21	172 ± 32.1 *
PAI-1	1 ± 0.21	283 ± 26.8 *
Inflammation		
TNF-α	1 ± 0.35	24.2 ± 7.99 *
MCP-1	1 ± 0.20	453 ± 48.8 *
gp91phox	1 ± 0.32	15.8 ± 1.99 *

Expression of mRNA was measured by RT-PCR method. Values are means ± SEM of 5 to 8 samples per each group.

* $p<0.01$ vs. $XOR^{+/+}$ mice. HMG-CoA: 3-hydroxy-3-methylglutaryl coenzyme A synthase, FAS: fatty acid synthase SREBP-1c: sterol regulatory element-binding protein-1c, C/EBP: CCAAT/enhancer binding protein, PPAR: peroxisome proliferator-activated receptor, TGF-β: transforming growth factor-β, α-SMA: α-smooth muscle actin, PAI-1: plasminogen activator inhibitor-1, TNF-α: tumor necrosis factor-α, MCP-1: monocyte chemoattractant protein-1